Hexokinases inhibit death receptor–dependent apoptosis on the mitochondria

Joachim Lauterwasser[a,1], Franziska Fimm-Todt[a,1], Aline Oelgeklaus[a,b,c,d,1], Annabell Schreiner[a], Kathrin Funk[a,d], Hugo Falquez-Medina[a,b], Ramona Klesse[a,d], Günther Jahreis[e], Ralf M. Zerbes[a], Katelyn O'Neill[f,g], Martin van der Laan[a,h], Xu Luo[f,g], and Frank Edlich[a,b,2]

[a]Institute for Biochemistry and Molecular Biology, Faculty of Medicine, University of Freiburg, 79104 Freiburg, Germany; [b]Veterinary Physiological Chemical Institute, Faculty of Veterinary Medicine, University of Leipzig, 04103 Leipzig, Germany; [c]Spemann Graduate School of Biology and Medicine, 79104 Freiburg, Germany; [d]Faculty of Biology, University of Freiburg, 79104 Freiburg, Germany; [e]Institute for Biochemistry and Biotechnology, University of Halle, 06120 Halle, Germany; [f]Eppley Institute for Research in Cancer and Allied Diseases, Fred & Pamela Buffett Cancer Center, University of Nebraska Medical Center, Omaha, NE 68198; [g]Department of Pathology and Microbiology, University of Nebraska Medical Center, Omaha, NE 68198; and [h]Medical Biochemistry and Molecular Biology, Saarland University, D-66421 Homburg, Germany

Edited by Junying Yuan, Shanghai Institute of Organic Chemistry, Shanghai, China, and approved July 12, 2021 (received for review October 12, 2020)

Death receptor–mediated apoptosis requires the mitochondrial apoptosis pathway in many mammalian cells. In response to death receptor signaling, the truncated BH3-only protein BID can activate the proapoptotic BCL-2 proteins BAX and BAK and trigger the permeabilization of the mitochondria. BAX and BAK are inhibited by prosurvival BCL-2 proteins through retrotranslocation from the mitochondria into the cytosol, but a specific resistance mechanism to truncated BID-dependent apoptosis is unknown. Here, we report that hexokinase 1 and hexokinase 2 inhibit the apoptosis activator truncated BID as well as the effectors BAX and BAK by retrotranslocation from the mitochondria into the cytosol. BCL-2 protein shuttling and protection from TRAIL- and FasL-induced cell death requires mitochondrial hexokinase localization and interactions with the BH3 motifs of BCL-2 proteins but not glucose phosphorylation. Together, our work establishes hexokinase-dependent retrotranslocation of truncated BID as a selective protective mechanism against death receptor–induced apoptosis on the mitochondria.

apoptosis | BCL-2 proteins | BH3-only proteins

The programmed cell death apoptosis protects multicellular organisms from harmful or infected cells (1–3). Apoptosis can be induced by death receptor signaling in response to death receptor ligands, such as FasL and TRAIL (4). Activated death receptors trigger a cytosolic cascade of apoptosis-specific cysteine proteases, termed caspases (5). Cytotoxic T cells eliminate tumor cells through this mechanism, elicited or amplified by immunotherapy. In mammalian cells, death receptor ligand–induced apoptosis usually requires the mitochondrial apoptosis pathway (6). Caspases engage mitochondrial apoptosis through the cleavage of the BCL-2 homology domain 3 (BH3)–only protein BID (7). Truncated BID (tBID) can inhibit prosurvival BCL-2 proteins and thus activate the proapoptotic BCL-2 proteins BAX and BAK (8–10). Once BAX and BAK are active, they release proteins from the intermembrane space by permeabilizing the outer mitochondrial membrane (OMM), thereby committing the cell to apoptotic fate through the caspase cascade. Prosurvival BCL-2 proteins inhibit BAX and BAK by constant retrotranslocation from the mitochondria into the cytosol (11–13). This dynamic shuttling of BAX and BAK determines the relevant protein pool on the OMM and, consequently, the cellular response to apoptosis stimulation (14, 15). BH3-only proteins, such as tBID, inhibit BAX/BAK retrotranslocation. Therefore, death receptor signaling shifts BAX and BAK toward the mitochondria through tBID and induces OMM permeabilization.

Hexokinases catalyze the first step of the glucose metabolism to produce glucose-6-phosphate (G-6P), which can be funneled into ATP production (glycolysis), storage (glycogenesis), and biosynthesis (pentose phosphate pathway and hexosamine pathway). The four human isoforms of hexokinases play, therefore, important roles in the regulation of anabolic and catabolic processes in human cells. Hexokinases have been also observed to protect cells from apoptosis (16–18). Ectopic HK2 expression has protective effects in different cell types (19–21). HK2 up-regulation is associated with poor prognosis in human brain metastases of breast cancer and human glioblastoma (22, 23). HK2 expression levels have been linked to tumor grade and mortality in hepatocellular carcinoma (24). Anti-apoptotic effects have been attributed to the HK1 binding to mitochondria, in particular to the voltage-dependent anion channel (VDAC) (25). Mitochondrial HK2 has also been suggested to antagonize proapoptotic BCL-2 family proteins (26). Here, we show that mitochondrial HK1 and HK2 selectively retrotranslocate tBID, BAX, and BAK from the mitochondria and, therefore, inhibit death receptor–mediated apoptosis on the mitochondria.

Results

Hexokinases Accelerate the Retrotranslocation of BAX and BAK. We used a BioID candidate approach labeling transient interaction partners with biotin to identify proteins involved in BAX retrotranslocation (Fig. 1*A*) (27). Previously suggested interaction partners, such as hexokinases, creatine kinases, peripheral benzodiazepine receptor, or CHCHD2, were included (Fig. 1*B*). This approach identified the hexokinases HK1 and HK2 in addition to BCL-x_L and expected auto-labeling of BAX (Fig. 1*B* and *SI Appendix*, Fig. S1). Transient interactions between hexokinases and BAX could influence BAX regulation. We, therefore, analyzed GFP-BAX retrotranslocation with and without ectopic hexokinase

Significance

Receptor–ligand interactions on the cell surface or intrinsic stress signals can commit mammalian cells to apoptosis. In this study, we discover how hexokinases confer resistance to receptor-mediated apoptosis through specific inhibition of B-cell lymphoma 2 (BCL-2) proteins. Hexokinases retrotranslocate activator and effector BCL-2 proteins from the mitochondria into the cytosol. Hexokinase-dependent BCL-2 protein retrotranslocation can protect cells from apoptosis despite death receptor signaling.

Author contributions: F.E. designed research; J.L., F.F.-T., A.O., A.S., K.F., H.F.-M., R.K., and R.M.Z. performed research; G.J., K.O., and X.L. contributed new reagents/analytic tools; J.L., A.O., and M.v.d.L. analyzed data; and F.E. wrote the paper.

The authors declare no competing interest.

This article is a PNAS Direct Submission.

This open access article is distributed under Creative Commons Attribution-NonCommercial-NoDerivatives License 4.0 (CC BY-NC-ND).

[1]J.L., F.F.-T., and A.O. contributed equally to this work.

[2]To whom correspondence may be addressed. Email: frank.edlich@uni-leipzig.de.

This article contains supporting information online at https://www.pnas.org/lookup/suppl/doi:10.1073/pnas.2021175118/-/DCSupplemental.

Published August 12, 2021.

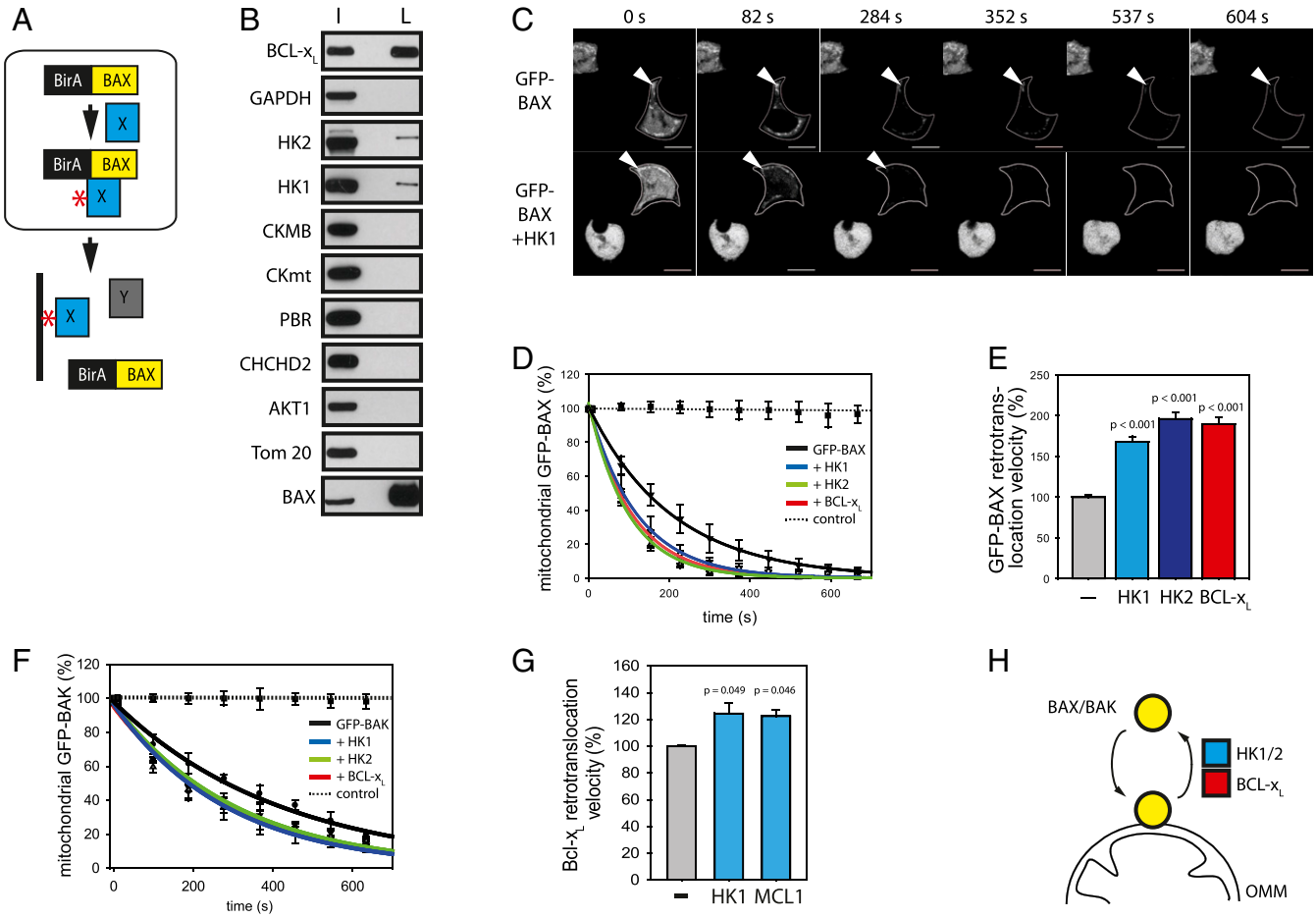

Fig. 1. Hexokinases accelerate BAX/BAK retrotranslocation. (*A*) BirA-BAX expression (yellow) in cells (square) labeled transient BAX interaction partners (X, blue) with biotin (red star). BAX-interacting proteins (X, blue) and unlabeled proteins (Y, gray) were separated by a biotin affinity matrix (solid line). (*B*) Hexokinases HK1 and HK2 and the prosurvival BCL-2 protein BCL-x_L were identified as transient BAX-binding proteins (input [I] and labeled fraction [L]) by Western blot. BirA-BAX was analyzed using anti-myc antibodies. $n = 3$. (*C*) FLIP measurements of GFP-BAX in the absence (*Top*) and the presence of overexpressed HK1 (*Bottom*) diminished GFP-BAX fluorescence in the cytosol of targeted cells (circled) completely after 82 s, and GFP-BAX was detected on the mitochondria (arrowheads). Time is in seconds. (Scale bars [white bar] = 10 μm.) (*D*) FLIP of GFP-BAX without (solid black line) and with overexpressed HK1 (blue), HK2 (green), and BCL-x_L (red) ± SEM from 132 (–), 137 (+HK1), 118 (+HK2), or 125 (+BCL-x_L) region of interest (ROI) measurements. Fluorescence of the neighboring cell is shown as control (broken line). (*E*) GFP-BAX retrotranslocation velocity without (gray, –) and with overexpressed HK1 (light blue), HK2 (dark blue), or BCL-x_L (red) ± SD *P* values according to one-way ANOVA. (*F*) FLIP of GFP-BAK without (solid black line) and with overexpressed HK1 (blue), HK2 (green), and BCL-x_L (red, obscured by HK1/2) ± SEM from 92 (–), 88 (+HK1), 93 (+HK2), or 94 (+BCL-x_L) ROI measurements. Fluorescence of the neighboring cell served as control (broken line). (*G*) GFP-BCL-x_L retrotranslocation velocity without (gray, –) and with overexpressed HK1 or MCL-1 ± SD *P* values according to one-way ANOVA. (*H*) Transient interactions with prosurvival BCL-2 proteins (e.g., BCL-x_L, red) or HK1/2 (blue) accelerate retrotranslocation of BAX/BAK (yellow) from the OMM into the cytosol.

expression using fluorescence loss in photobleaching (FLIP) (28). In brief, repeated cycles of bleaching diminish cytosolic GFP-BAX fluorescence, and imaging between bleaching cycles characterizes the mitochondrial GFP-BAX pool and thus retrotranslocation kinetics (Fig. 1 *C* and *D*). Ectopic expression of HK1/2 accelerated BAX retrotranslocation to the same extend as ectopic BCL-x_L expression with the corresponding endogenous proteins present (Fig. 1 *D* and *E*). BAX retrotranslocation kinetics with a low margin of error and the microscopic analysis of mCherry-BAX and HK1-GFP coexpression showed that cells ectopically expressing mCherry-BAX also expressed HK1-GFP (*SI Appendix*, Fig. S2). Based on hexokinase-dependent BAX retrotranslocation and similar regulation of BAX and BAK, we tested the potential of hexokinases to participate in BAK retrotranslocation. BAK shuttling from the mitochondria into the cytosol was accelerated by ectopic HK1/2 and BCL-x_L expression to comparable velocity (Fig. 1*F* and *SI Appendix*, Fig. S3). Therefore, hexokinases accelerate the retrotranslocation of BAX and BAK. HK1 also accelerated BCL-x_L retrotranslocation similar to the anti-apoptotic BCL-2 protein MCL-1 with comparable BAX retrotranslocation activity, suggesting interdependency between proteins retrotranslocation BAX and BAK (Fig. 1*G*). In addition, BCL-x_L overexpression shifted HK1/2 to the cytosol (*SI Appendix*, Fig. S4). Despite structural and functional differences, hexokinases and prosurvival BCL-2 proteins participated in BAX/BAK retrotranslocation (Fig. 1*G*).

Mitochondrial Hexokinases Inhibit Commitment to Apoptosis. Hexokinase-dependent BAX/BAK retrotranslocation could link the glucose metabolism to mitochondrial apoptosis regulation. We analyzed the influence of glucose phosphorylation on BAX shuttling using the in-organelle BAX retrotranslocation assay (29). Application of the glycolysis inhibitor 2-Deoxy-D-glucose (2-DG) to HCT116 cells or the presence of the hexokinase inhibitor G-6P did not change endogenous BAX shuttling from isolated mitochondria (Fig. 2 *A* and *B* and *SI Appendix*, Figs. S5 and S6). GFP-BAX shuttling was also accelerated by catalytically

compromised HK1 D657A or HK2 D209/657A (Fig. 2 *C* and *D*). These results suggest glucose phosphorylation-independent BAX retrotranslocation.

However, reduced BAX retrotranslocation rates due to catalytically impaired hexokinases may indicate reduced mitochondrial hexokinase presence (*SI Appendix*, Fig. S7). HK2-GFP largely colocalized with mitochondria (Pearson's coefficient $r = 0.846$), whereas HK2-GFP D209/657A was shifted to the cytosol (Pearson's coefficient $r = 0.633$). Mitochondrial hexokinase localization can be inhibited by peptides mimicking the N-terminal transmembrane domains (TMDs) (30). Hexokinase TMD-derived peptides reduced BAX shuttling velocity and the amount of shuttled BAX (Fig. 2 *E* and *F*). Consequently, hexokinase TMD-derived peptides induced OMM permeabilization in a concentration-dependent manner by shifting hexokinases from mitochondria until BAX and BAK were active (Fig. 2*G* and *SI Appendix*, Figs. S8–S10). The induction of OMM permeabilization by hexokinase TMD-derived peptides parallels BCL-x_L TMD effects (*SI Appendix*, Fig. S11). Notably, the BCL-x_L TMD can bind BAX molecules and decrease their likelihood of being activated (31) but also compete with full-length

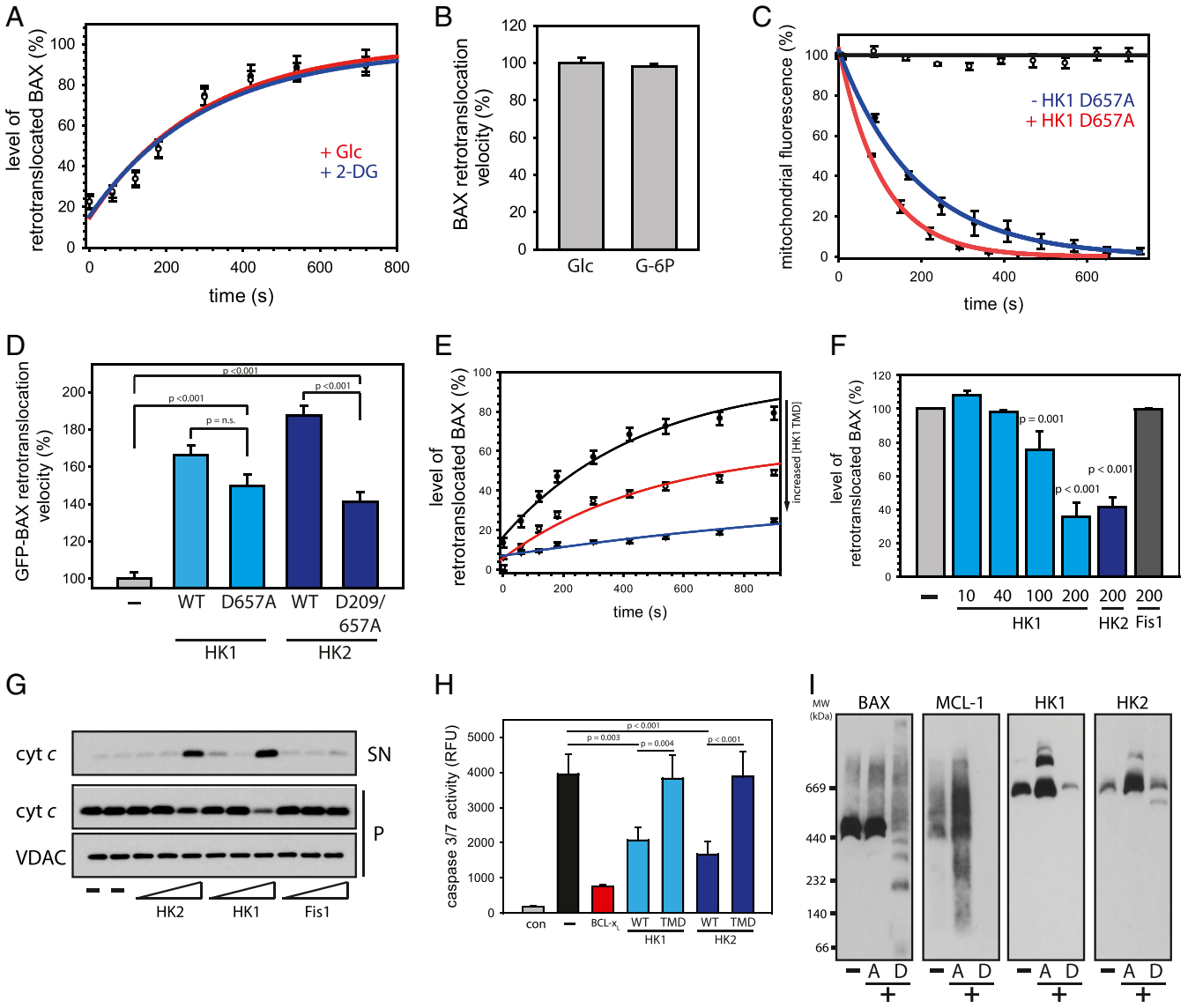

Fig. 2. Mitochondrial hexokinase inhibits apoptosis. (*A*) Retrotranslocation of BAX from isolated mitochondria after pretreatment of cells with either glucose (Glc, red) or 2-deoxy-D-glucose (2-DG, blue). $n = 3$. (*B*) BAX shuttling velocity from isolated mitochondria in the presence of Glc or G-6P. $n = 3$. (*C*) FLIP of GFP-BAX without (blue line) and with overexpressed HK1 D657A (red line) ± SEM from 122 (–) or 117 (+HK1 D657A) ROI measurements. The neighboring cell served as control (solid black line). (*D*) GFP-BAX retrotranslocation without (gray, –) and with overexpressed HK1 (light blue) wild-type or D657A as well as HK2 (dark blue) wild-type or D209/657A ± SD *P* values according to one-way ANOVA. (*E*) BAX shuttling from isolated mitochondria without (•, black) or with 100 (○, red) or 200 μM (▼, blue) of HK1 TMD peptide. (*F*) BAX retrotranslocation from isolated mitochondria without (light gray, –) or with HK1 TMD peptide (light blue) or 200 μM HK2 TMD peptide (dark blue) or 200 μM Fis1 TMD peptide (dark gray, negative control). (*G*) OMM permeabilization of isolated mitochondria without (–) or with 25, 100, or 250 μM of either HK1, HK2, or Fis1 TMD peptide, monitored by cyt *c* release into the supernatant (SN). The mitochondrial fraction (P) and VDAC served as controls. (*H*) Caspase 3/7 activity in HCT116 BCL-2allKO cells with (black, –) and without (gray) ectopic BAX expression with and without overexpressed BCL-x_L (red), HK1 (light blue, either wild-type or N-terminal TMD), or HK2 (dark blue, either wild-type or N-terminal TMD) ± SD. $n = 3$. *P* values according to one-way ANOVA. (*I*) BN-PAGE of isolated mitochondria with (+) or without (–) apoptosis induction through BCL-2/BCL-x_L inhibition by the BH3 mimetic ABT-737of attached (A) and detached (D) and therefore apoptotic cells. The apparent molecular weight (MW) is indicated.

https://doi.org/10.1073/pnas.2021175118

BCL-x_L for BAX binding at high concentrations and therefore favor BAX activation (32). In parallel, TMD-derived peptides competed with endogenous hexokinases and interfere with hexokinase-dependent BAX/BAK inhibition.

Hexokinase TMDs alone are insufficient to inhibit BAX/BAK. Therefore, ectopic expression of either HK1 or HK2 but not the respective TMDs inhibited GFP-BAX expression-mediated apoptosis in HCT116 cells lacking 17 members of the BCL-2 family (Fig. 2*H* and *SI Appendix*, Fig. S12) (33). The blue native polyacrylamide gel electrophoresis (PAGE) analysis of mitochondrial complexes shows further similarities between HK1/2 and prosurvival BCL-2 proteins: mitochondrial complexes of BCL-x_L, HK1, and HK2 depended on VDAC2 and accumulated in attached cells in the presence of apoptotic stimuli (Fig. 2*I* and *SI Appendix*, Figs. S13–S15) (29). However, BAX/BAK retrotranslocating proteins were not present in the same complexes and therefore lack stable interactions.

Hexokinase binding to VDAC can be inhibited by the small molecule Clotrimazole (CLZ) (34). VDAC inhibitors such as CyclosporinA (CsA) and 4,4′-diisothiocyanostilbene-2,2′-disulfonic acid (DIDS) also alter mitochondrial hexokinase association. CsA, like CLZ, shifted HK1 from the mitochondria and increased OMM permeabilization, whereas DIDS had the adverse effects (*SI Appendix*, Figs. S16 and S17). Therefore, mitochondrial hexokinases but not glucose phosphorylation accelerate BAX/BAK retrotranslocation and confer apoptosis resistance.

Hexokinase-Dependent BCL-2 Protein Shuttling Inhibits Death Receptor–Mediated Apoptosis. Inhibition of OMM permeabilization by mitochondrial hexokinases suggests that hexokinase localization regulates apoptosis. Predominantly cytosolic hexokinases in the presence of either CLZ or CsA should increase susceptibility to apoptosis, whereas increased mitochondrial hexokinase in the

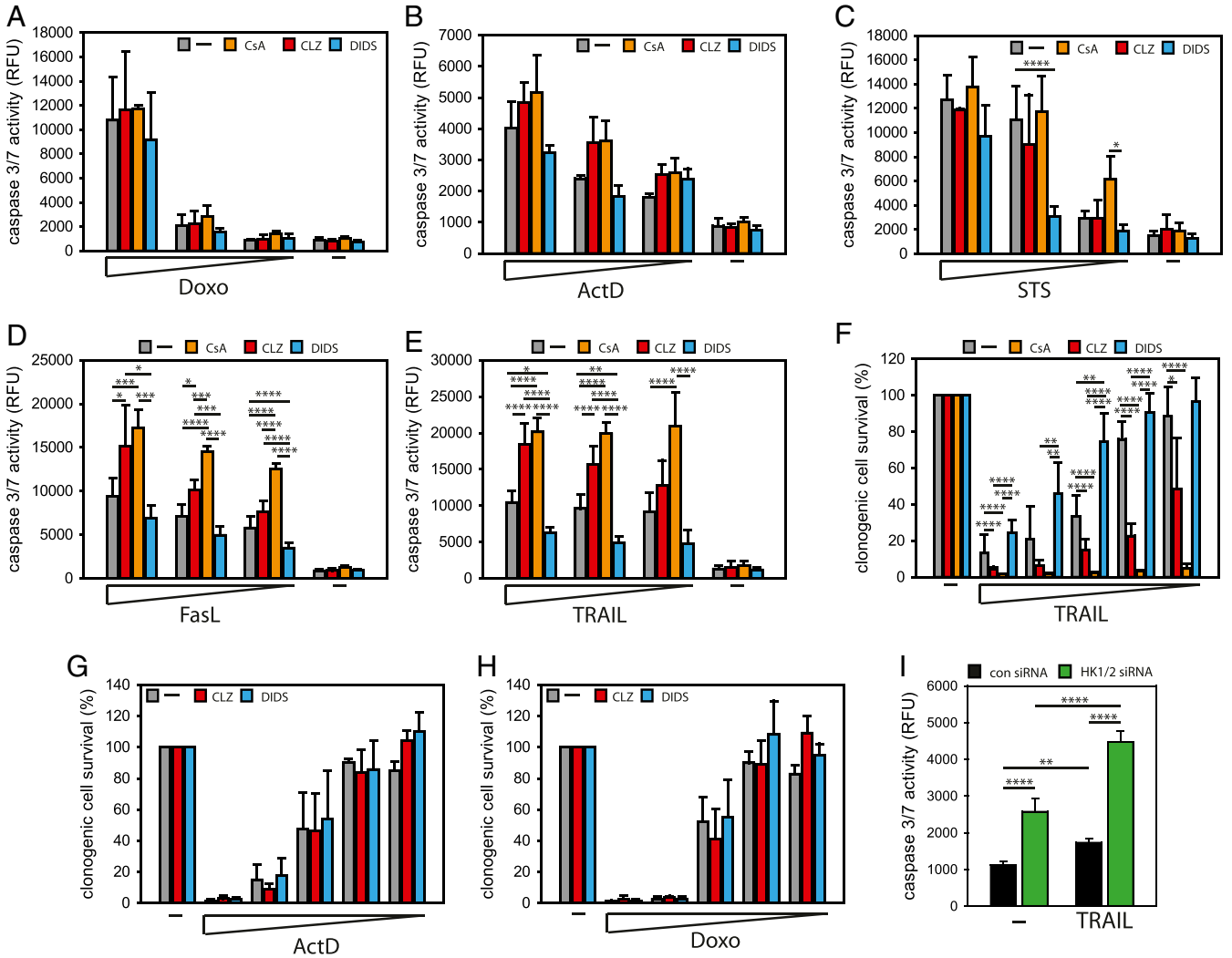

Fig. 3. Mitochondrial hexokinases protect cells from death receptor-mediated apoptosis. (*A–E*) Caspase 3/7 activity after apoptosis induction by Doxorubicin (Doxo, *A*), ActinomycinD (ActD, *B*), Staurosporine (STS, *C*), FasL (*D*), or TRAIL (*E*) without (DMSO, gray, –) or with CLZ (red), CsA (orange), or DIDS (blue) ± SD. $n = 3$. *P* values are> 0.001 (****), 0.001 to 0.005 (***), 0.005 to 0.01 (**), and 0.01 to 0.05 (*) according to one-way ANOVA. (*F–H*) Clonogenic HCT116 cell survival following TRAIL, Actinomycin D (ActD, *G*), or Doxorubicin (Doxo, *H*) treatment without (DMSO, gray, –) or with CLZ (red), CsA (orange), or DIDS (blue) ± SD. $n = 3$. *P* values are > 0.001 (****), 0.001 to 0.005 (***), 0.005 to 0.01 (**), and 0.01 to 0.05 (*) according to one-way ANOVA. (*I*) Caspase 3/7 activity in the presence of HK1/2 siRNA (green) or control siRNA (black) without (–) and with apoptosis induction by TRAIL ± SD. $n = 3$. *P* values are > 0.001 (****) and 0.005 to 0.01 (**) according to one-way ANOVA. Noteworthy, HK1/2 siRNA results in a predominant reduction of HK1 levels, while expression regulation of HK2 diminishes HK2 level reduction in the presence of HK1 siRNA. Functional redundancy of HKs suggests similar effects by level reduction of both hexokinases.

presence of DIDS is anticipated to reduce cellular apoptosis predisposition. However, Doxorubicin-induced apoptosis was not influenced by altered hexokinase localization (Fig. 3*A*). Similarly, neither predominantly mitochondrial hexokinase localization in the presence of DIDS nor largely cytosolic localization of hexokinases with CLZ or CsA produced a tendency in Actinomycin D– or Staurosporine-induced apoptosis (Fig. 3 *B* and *C*). Strikingly, increased cytosolic hexokinase localization caused enhanced caspase activation when apoptosis was induced by the death receptor ligand FasL (Fig. 3*D*). In addition, hexokinase shifted to the mitochondria resulted in the tendency toward reduced apoptosis commitment. Therefore, hexokinase localization could specifically regulate death receptor–induced apoptosis.

TRAIL-induced apoptosis supports this possibility: increased cytosolic hexokinase localization resulted in enhanced caspase activation by the death receptor ligand, while increased mitochondrial hexokinase protected cells from TRAIL (Fig. 3*E*). Shifting hexokinase to the mitochondria also protected U2OS cells against TRAIL-induced apoptosis, while increased cytosolic hexokinase localization amplified apoptotic response (*SI Appendix*, Fig. S18). In parallel to HCT116 cells, mitochondrial hexokinase localization failed to protect U2OS cells from intrinsic apoptotic stress induced by Actinomycin D or Doxorubicin and cytosolic hexokinase did not produce increased apoptosis as well (*SI Appendix*, Fig. S19).

We then tested whether differences in caspase activity changed apoptosis kinetics or translated into altered cell fates by assaying clonogenic survival. Again, TRAIL-induced apoptosis was significantly enhanced when hexokinases were shifted toward the cytosol and increased mitochondrial hexokinase produced a tendency to greater apoptosis resistance (Fig. 3*F*). In contrast, hexokinase localization did not influence cell death in response to intrinsic stress induced by Actinomycin D or Doxorubicin (Fig. 3 *G* and *H*). The role of hexokinases in apoptosis inhibition is supported by small interfering RNA (siRNA)-induced apoptosis (*SI Appendix*, Figs. S20 and S21). TRAIL-induced apoptosis is further enhanced when HK1/HK2 expression is diminished (Fig. 3*I* and *SI Appendix*, Figs. S22 and S23). Therefore, mitochondrial hexokinases protect cells specifically from death receptor–mediated apoptosis.

Hexokinase-Dependent Retrotranslocation Inhibits tBID. Receptor-mediated apoptosis is linked to the mitochondrial pathway through the cleavage of the BH3-only protein BID. We tested the potential inhibition of tBID-dependent apoptosis by hexokinases, using a defined setting with BAX, BCL-x_L, and tBID or the BH3-only protein BIM as the only present BCL-2 proteins in BCL-2allKO cells. Overexpression of BAX alone commits BCL-2allKO cells to apoptosis, preventing BAX expression to levels detectable by Western blot (33). Therefore, additional BCL-x_L expression is required for cell survival and BAX expression to detectable levels. When only tBID could induce apoptosis, a CLZ-mediated hexokinase shift toward the cytosol profoundly enhanced commitment to apoptosis (Fig. 4 *A* and *B* and *SI Appendix*, Fig. S24). Hexokinases could only partially inhibit overexpressed BAX in BCL-2allKO cells (Fig. 4*C*). Reduced inhibition of BAX-induced caspase activity, poly ADP ribose polymerase (PARP) cleavage and loss in membrane potential by HK1/2 compared to BCL-x_L shows lower potency of hexokinases to inhibit BAX. Reduced BAX inhibition by HK1/2 also explains lower BAX expression when only hexokinases are present (*SI Appendix*, Figs. S25–S27). In parallel to BAX/BAK inhibition by hexokinases, protection against tBID-induced cell death required mitochondrial association of full-length hexokinase (Fig. 4 *D–F* and *SI Appendix*, Figs. S27). The discrepancy between hexokinase- and BCL-2 protein–dependent cell protection and accelerated BAX/BAK shuttling (Fig. 1) suggests the involvement of an additional apoptosis inhibition mechanism. Since tBID binds the OMM (35), we tested the effect of HK1 on BH3-only protein shuttling. Strikingly, HK1 accelerates the retrotranslocation of tBID, while BCL-x_L inhibits tBID shuttling from the mitochondria (Fig. 5 *A–C*). In contrast, hexokinases did not influence BIM or PUMA shuttling (Fig. 5 *D–I*). Therefore, mitochondrial hexokinases inhibit apoptosis by two different shuttling mechanisms: effector inhibition through BAX/BAK retrotranslocation and activator inhibition by specifically retrotranslocating mitochondrial tBID.

Hexokinases form BAX/BAK and tBID Retrotranslocation Complexes Dependent on BH3 Binding. Hexokinase-dependent retrotranslocation suggests that mitochondrial localization and specific interactions between hexokinase and BCL-2 proteins are required for BCL-2 protein shuttling. Shifting hexokinases toward the cytosol inhibited hexokinase-dependent tBID retrotranslocation (Fig. 6 *A* and *B*). This parallels BAX retrotranslocation (Fig. 6*C*). The BH3 mimetic ABT-737 also reduced tBID retrotranslocation but has no further effect in the presence of CLZ. ABT-737-mediated inhibition of tBID retrotranslocation could result from competition between the BH3 mimetic and the BH3-only protein for hexokinase binding. The binding of hexokinases to the BH3 motif could explain why hexokinases can retrotranslocate BAX, BAK, and tBID, while differences in the BH3 motif could prevent BIM shuttling. We tested this hypothesis by analyzing potential interactions between HK1 and the BH3-only proteins tBID and BIM (Fig. 6*D*). tBID and BIM formed complexes with HK1. BCL-x_L increased the pool of tBID-bound HK1. CLZ, on the other hand, prevented interactions between both BH3-only proteins and HK1, but BCL-x_L-binding to tBID and BIM remained undisrupted (Fig. 6*D*). The inhibitory effect of CLZ, CsA, and ABT-737 on transient interactions between HK1 and BirA-tBID corroborates disruption of hexokinase-dependent apoptosis inhibition by these small molecules (Fig. 6*E*). Interestingly, hexokinase localization affected transient interactions with BCL-x_L similarly that could play a role in the interdependent regulation of proteins regulating BAX (Fig. 1) but not retrotranslocation of BAX or tBID (Figs. 4 and 5). The role of the BH3 motif in hexokinase interactions with the BCL-2 family is corroborated by reduced interactions between hexokinases and BAX variants lacking the BH3 motif or containing the triple alanine substitution 63–65A (Fig. 6*F*). Together the retrotranslocation of BAX, BAK, and tBID, the inhibitory effect of ABT-737 on interactions, binding to BID, BIM, and BAX, and the disruptive effect of BAX BH3 variants on hexokinases suggest that hexokinases interact via the BH3 motif with BCL-2 proteins. Mitochondrial hexokinases reduce the cellular predisposition to BAX/BAK activation and inhibit death receptor–mediated apoptosis via effector retrotranslocation of BAX/BAK and shuttling of the activator tBID (Fig. 6*F*).

Discussion

Hexokinase-dependent retrotranslocation of tBID, BAX, and BAK from the mitochondria into the cytosol is an example of dynamic BCL-2 protein shuttling from the OMM by non–BCL-2 proteins. Through selective inhibition of tBID, hexokinase-dependent retrotranslocation is a direct countermeasure to mitochondrial apoptosis in response to death receptor signaling. Death ligand–induced mitochondrial apoptosis by cytotoxic T cells requires inhibition of tBID and BAX/BAK retrotranslocation in addition to caspase-mediated BID cleavage. Therefore, hexokinase-dependent retrotranslocation contributes to cell-to-cell differences in apoptosis induction and increases resistance to TRAIL and FasL. tBID-specific inhibition by hexokinases also illuminates the previously recognized cell type–specific differential apoptosis induction by tBID and BIM (36, 37). Differences in tBID/BIM activities could manifest in some tissues but be absent from others (38), depending on the tBID retrotranslocation rate. Accelerated BAX/BAK retrotranslocation by ectopic hexokinase expression also supports a "primed to death"

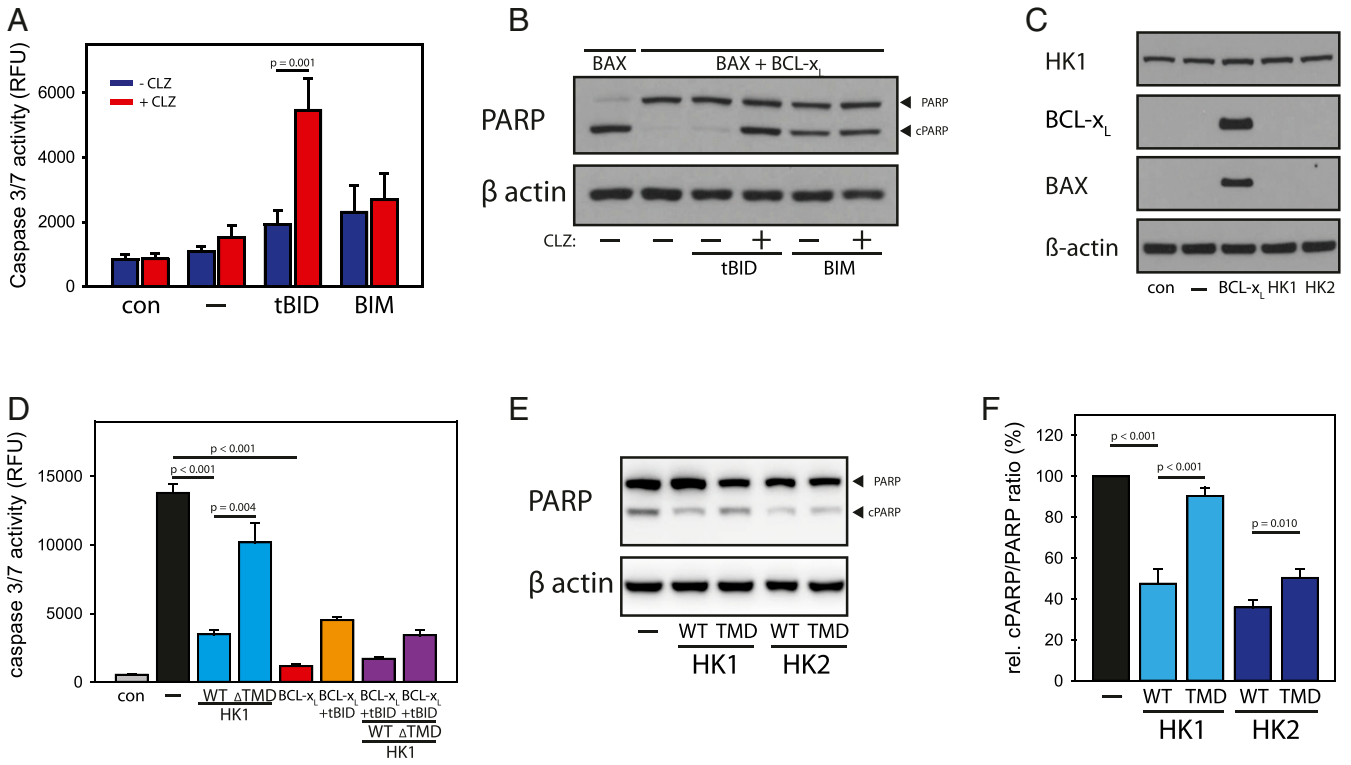

Fig. 4. Mitochondrial hexokinases inhibit tBID-dependent apoptosis. (*A*) Caspase 3/7 activity in HCT116 BCL-2allKO cells following expression (mock – con) of BAX, BCL-x_L (–), and either tBID or BIM without (blue) or with CLZ (red) ± SD. $n = 3$. *P* values are according to one-way ANOVA. (*B*) PARP cleavage of cells in *A* after expression of BAX, BCL-x_L, and either tBID or BIM without (DMSO, –) or with CLZ. β-actin served as control. $n = 3$. (*C*) Protein levels of HK1 (endogenous and ectopically expressed), BCL-x_L, and GFP-BAX in HCT116 BCL-2allKO ectopically expressing GFP-BAX alone (–), GFP-BAX and BCL-x_L (BCL-x_L), GFP-BAX and HK1 (HK1), and GFP-BAX and HK2 (HK2). $n = 3$. β-actin served as control. (*D*) Caspase 3/7 activity measurement in HCT116 BCL-2allKO cells without (gray) or with overexpressed GFP-BAX in the absence (black, –) or the presence of HK1 (light blue, wild-type, or lacking the N-terminal TMD [ΔTMD]) or BCL-x_L (red) ± SD. Increased caspase activity in the presence of ectopic tBID expression in HCT116 BCL-2allKO cells over-expressing GFP-BAX and BCL-x_L (orange) is decreased by additional overexpression of HK1 (purple, wild-type, or lacking the N-terminal TMD [ΔTMD]). $n = 3$. *P* values according to one-way ANOVA. (*E*) PARP cleavage of HCT116 BCL-2allKO cells over-expressing GFP-BAX, BCL-x_L, and tBID in the absence (–) or the presence of either overexpressed HK1 or overexpressed HK2 (wild-type or the N-terminal TMD [TMD]). β-actin served as control. $n = 3$. (*F*) Relative cleaved PARP/PARP ratio of samples depicted in *E*. *P* values are according to one-way ANOVA.

scenario (39, 40). Although hexokinases accelerate BAX/BAK shuttling, BAX/BAK retrotranslocation enhanced to the same rates by either hexokinases or prosurvival BCL-2 proteins involves hexokinase-dependent tBID retrotranslocation in turn freeing prosurvival BCL-2 proteins to shuttle BAX and BAK into the cytosol. Therefore, hexokinases play a central role in preventing receptor-mediated apoptosis predominantly by tBID retrotranslocation. BAX/BAK retrotranslocation is dominated by prosurvival BCL-2 proteins. Consequently, minor hexokinase-dependent effects were observed in intrinsic apoptosis that could result from direct BAX/BAK regulation or/and from shuttling unleashed tBID from the mitochondria. Since BID is also a substrate of caspase-2 and may thus mediate endoplasmic reticulum (ER) stress or DNA damage signaling to the mitochondria, hexokinase-dependence could contribute to tBID inhibition following intrinsic stress signals (41, 42). However, significant apoptosis inhibition by hexokinases occurred only in response to death receptor signaling.

Retrotranslocation of BCL-2 effector and activator proteins requires mitochondrial hexokinases that form VDAC2-dependent complexes like prosurvival BCL-2 proteins (29). Different BN-PAGE complex sizes suggest that stable complexes contain either hexokinases or prosurvival BCL-2 proteins. However, transient interactions during tBID/BAX/BAK retrotranslocation remain possible, as the presence of BCL-x_L influences tBID binding to hexokinases. These interactions could regulate the overall pool of proteins retrotranslocating BAX and BAK. Thereby, a stable mitochondrial BAX pool perhaps required for mitochondrial dynamics could be ensured. The nature of mitochondrial hexokinase complexes suggests the potential involvement of other factors and processes, including the cellular glucose metabolism. Nevertheless, the Glc-to–G-6P conversion is dispensable for hexokinase-dependent BCL-2 protein retrotranslocation. BCL-2–dependent BAX retrotranslocation involves interactions between its BH3 motif and the hydrophobic groove of prosurvival BCL-2 proteins (12). Hexokinase-dependent tBID/BAX/BAK retrotranslocation differs necessarily from this mechanism, because hexokinases lack a corresponding hydrophobic groove. However, our interaction studies and the shuttling of BAX, BAK, and tBID suggest the recognition of the BH3 motif by hexokinases. Additional interaction sites could discriminate between tBID and BIM during retrotranslocation, since BH3-binding might mediate interactions between BIM and hexokinases. Furthermore, binding of the BCL-2 protein to the cytosolic hexokinase domains are critical, as the hexokinase TMDs are insufficient to inhibit apoptosis. Inhibition of tBID shuttling by BCL-x_L further emphasizes the unique character of hexokinase-dependent tBID retrotranslocation. The reduced rate of tBID shuttling in the presence of BCL-x_L not only contrasts with BAX/BAK retrotranslocation but also supports the presence of OMM-embedded complexes between tBID and prosurvival BCL-2 proteins (43, 44). Our results support a role of embedded tBID/BCL-x_L in reducing the capacity of BCL-x_L to retrotranslocate BAX and BAK and thus increase apoptosis predisposition of the cell (14). The inverse scenario with embedded complexes inhibiting tBID-dependent BAX activation is unlikely

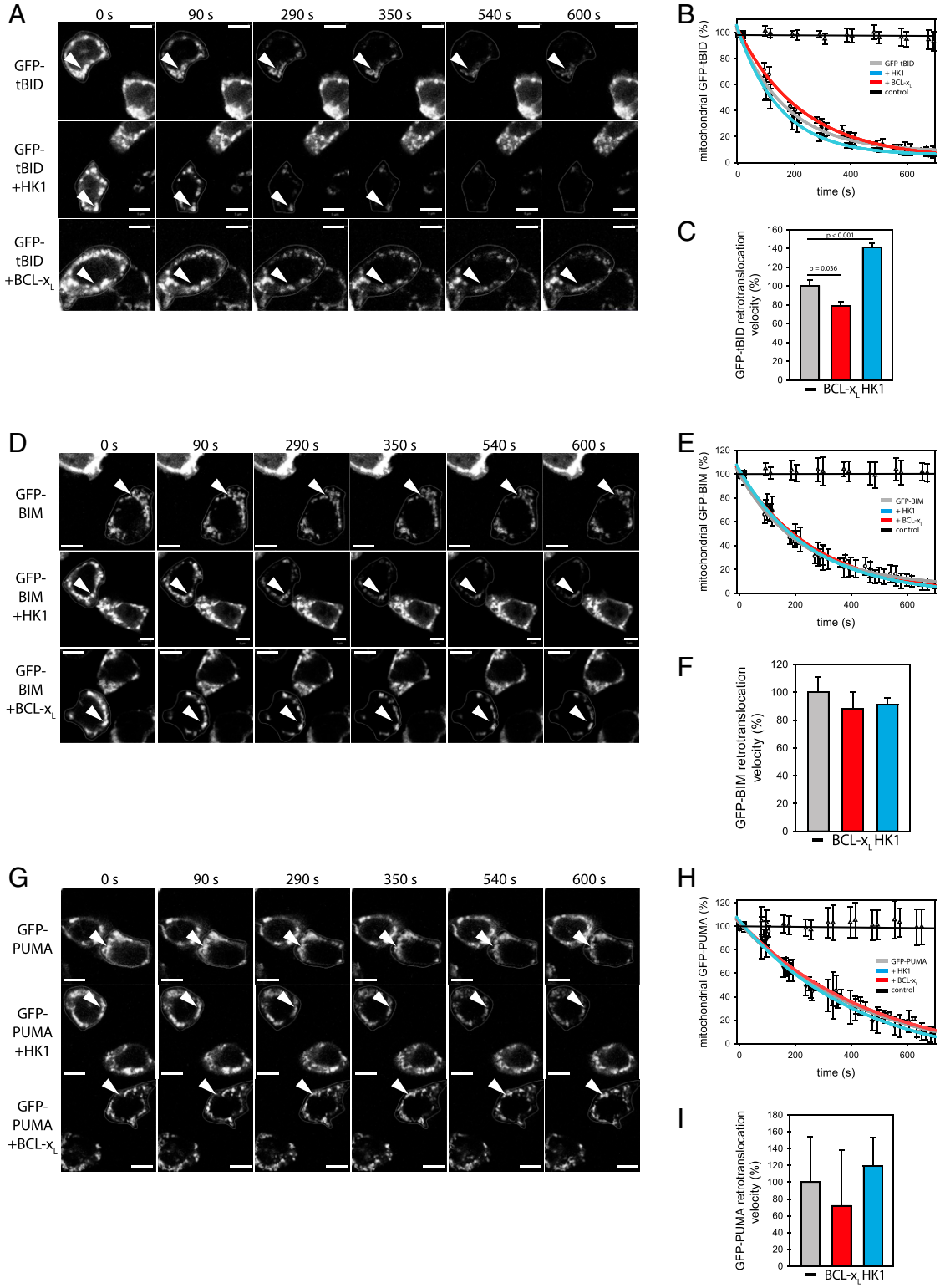

Fig. 5. Hexokinases selectively retrotranslocate tBID from the mitochondria. (*A*, *D*, and *G*) FLIP measurements of GFP-tagged tBID (*A*), BIM (*D*), or PUMA (*G*) in the absence (*Top*) and the presence of overexpressed HK1 (center) or BCL-x_L (*Bottom*) diminished GFP fluorescence in the cytosol of targeted cells (circled), and GFP-tagged BH3-only proteins were detected on the mitochondria (arrowheads). Time is in seconds. (Scale bar [white bar], 10 μm.) (*B, E,* and *H*) FLIP of GFP-tagged BH3-only proteins tBID (*B*), BIM (*E*), or PUMA (*H*)) without (gray) and with overexpressed HK1 (blue) and BCL-x_L (red). Fluorescence of the neighboring cell is shown as control (black). (*C*) Retrotranslocation of GFP-tBID in HCT116 BAX/BAK DKO cells with or without (gray, –) ectopically expressed HK1 (blue) or BCL-x_L (red) ± SD from 337 (–), 354 (+HK1), or 200 (+BCL-x_L) ROI measurements. $n = 3$. *P* values are according to one-way ANOVA. (*F*) GFP-BIM shuttling in HCT116 BAX/BAK DKO cells with or without (gray, –) overexpressed HK1 (blue) or BCL-x_L (red) ± SD from 182 (–), 180 (+HK1), or 138 (+BCL-x_L) ROI measurements. $n = 3$. (*I*) GFP-PUMA retrotranslocation in HCT116 BAX/BAK DKO cells with or without (gray, –) overexpressed HK1 (blue) or BCL-x_L (red) ± SD from 116 (–), 146 (+HK1), or 108 (+BCL-x_L) ROI measurements. $n = 3$.

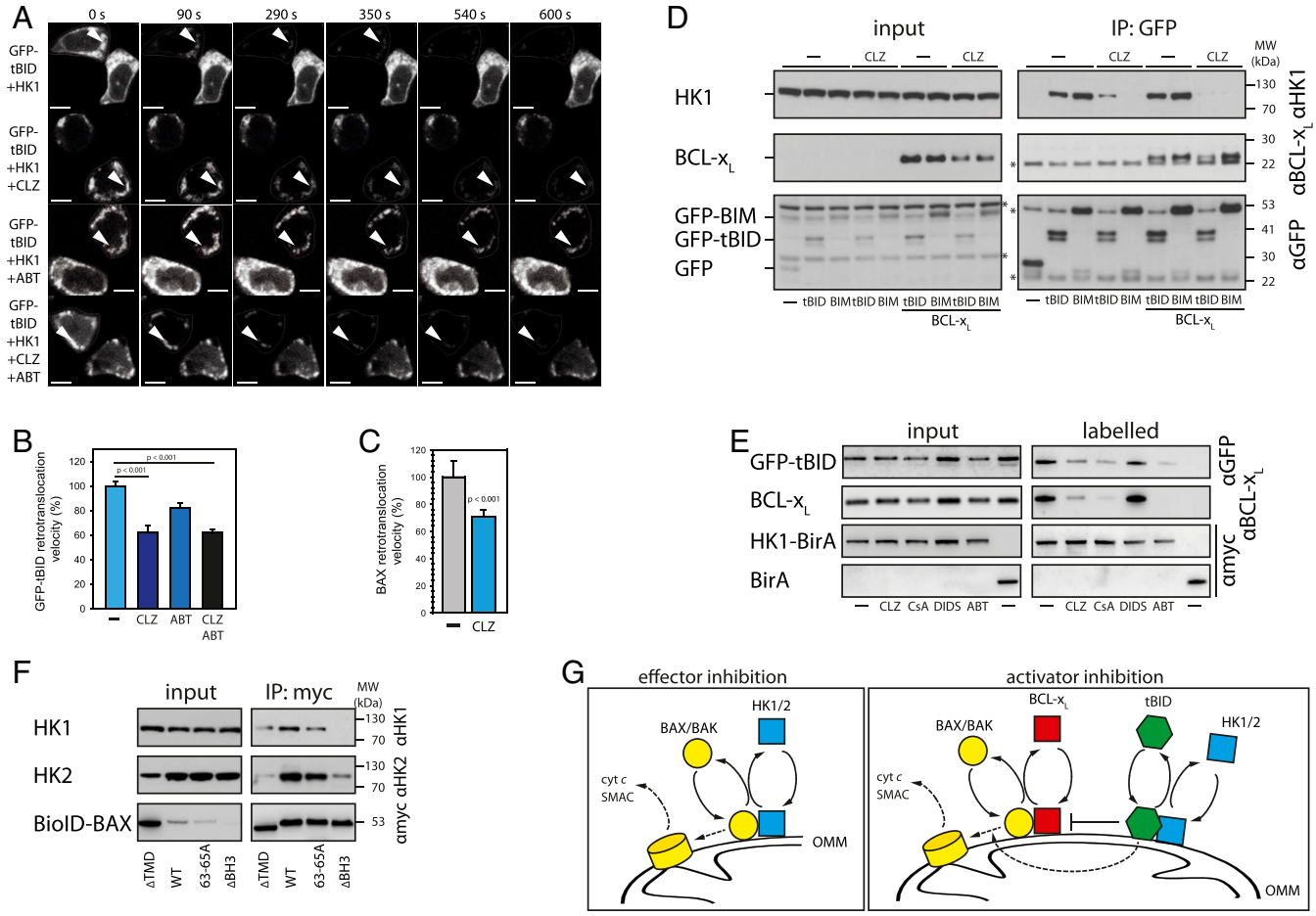

Fig. 6. Hexokinases interact with the BH3 motif during BCL-2 protein retrotranslocation. (*A*) FLIP measurements of GFP-tagged tBID in the presence of overexpressed HK1 without (*Top*) or with CLZ (second row), ABT-737 (third row), or both (*Bottom*) diminished GFP fluorescence in the cytosol of targeted cells (circled), and GFP-tagged tBID was detected on the mitochondria (arrowheads). Time is in seconds. (Scale bar [white bar], 10 μm.) (*B*) GFP-tBID shuttling in HCT116 BAX/BAK DKO cells with HK1 overexpression without (DMSO, –) or with CLZ (12 μM) and/or ABT-737 (10 μM, ABT) ± SD from 155 (–), 150 (+CLZ), 138 (+ABT), or 119 (+CLZ/ABT) ROI measurements. $n = 3$. *P* values are according to one-way ANOVA. *C*) GFP-BAX retrotranslocation in HCT116 BAX/BAK DKO cells without (DMSO, –) or with CLZ (12 μM) ± SD from 98 (–) or 116 (+CLZ) ROI measurements. $n = 3$. *P* values are according to one-way ANOVA. (*D*) Immunoprecipitation of either GFP-fused BIM, GFP-fused tBID, or GFP alone (–) in HCT116 BCL-2allKO cells analyzed for binding of endogenous HK1 or coexpressed BCL-x_L without (DMSO, –) and with CLZ treatment by Western blot. $n = 3$. (*E*) Ectopic expression of HK1-BirA or BirA alone labeled transient interaction partners with biotin in HCT116 cells. HK1-interacting proteins were analyzed for the presence of GFP-tBID and BCL-x_L without (DMSO, –) and with treatment with CLZ, CsA, DIDS, and ABT by Western blot. HK1-BirA and BirA was analyzed using anti-myc antibodies. $n = 3$. (*F*) IP of myc-fused BAX ΔTMD (lacking the C-terminal TMD), wild-type BAX, BAX 63–65A, or BAX ΔBH3 (lacking the BH3 domain) expressed in HCT116 BAX/BAK DKO cells and analyzed for binding of endogenous HK1 or HK2 by Western blot. $n = 3$. (*G*) Hexokinase-dependent BCL-2 protein retrotranslocation protects cells from BAX/BAK activity directly via effector inhibition and indirectly via activator inhibition. BAX/BAK (yellow) are retrotranslocated directly by hexokinases (blue), inhibiting BAX/BAK activation. Therefore, hexokinase activity prevents OMM permeabilization and commitment to apoptosis. In addition, specific inhibition of the activator tBID by hexokinases counteracts receptor-mediated apoptosis. Mitochondrial tBID (green) inhibits BAX/BAK (yellow) retrotranslocation into the cytosol by competing with BAX and BAK for prosurvival BCL-2 protein (red) interactions, forming OMM-embedded complexes with BCL-x_L. Mitochondrial HK1/2 (blue) selectively retrotranslocates tBID into the cytosol and counteracts BAX/BAK activation in response to death receptor–mediated apoptosis.

based on tBID inhibition by transient hexokinase-dependent retrotranslocation. Formation of embedded BCL-x_L complexes could be particularly prominent for tBID, as the BH3 mimetic ABT-737 does not inhibit BCL-x_L shuttling (12, 45). Hexokinase-dependent tBID retrotranslocation could play an important role in the clearance of particularly cancer cells by the immune system.

Materials and Methods

Cell Culture and Transfection. HCT116 wild-type cells, HCT116 BAX/BAK double knock-out (DKO) cells, HCT116 BCL-2allKO cells, and U2OS wild-type cells were cultured in McCoy's 5A medium supplemented with 10% heat-inactivated fetal bovine serum and 10 mM Hepes pH 7.3. Mouse embryonic fibroblasts (MEF) cells, MEF BAX/BAK DKO cells, and MEF VDAC2 knock-out (KO) cells were cultured in Dulbecco's Modified Eagle Medium (DMEM) and supplemented with 10% heat-inactivated fetal bovine serum and 10 mM Hepes pH7.3. All cell lines were cultured in 5% CO_2 at 37 °C in humified incubator.

Cells were seeded in 6-well plates or dishes and grown for 24 to 48 h. Cells were transfected using Turbofect reagent (Thermo Fisher Scientific) according to manufacturer's instructions. Empty vectors served as control in all comparative experiments. Cotransfections with pcDNA3.1, HK1, HK2, BCL-x_L, tBid, and Bim constructs were performed in 1:3 or 1:6 ratios. Cells were incubated for 4 to 6 h and then subjected to FLIP measurements, confocal imaging, or treatments. The experiments were performed with transient protein expression to avoid high protein levels resulting from stable or prolonged transient protein expression and resulting cell stress response (13).

FLIP Measurements. HCT116 Bax/Bak DKO cells were seeded on a Lab-TekTM chambered coverglass system (VWR) and incubated for 24 to 48 h in McCoy's 5A medium. Cells were transfected with GFP-tagged constructs containing the HK1, HK2, BAX, BAK, tBid, Bim, or Puma coding sequence (CDS) using

Turbofect reagent (Thermo Fisher Scientific) according to manufacturer's instructions.

FLIP experiments were performed as described previously (12). For each measurement, one cell expressing GFP-tagged protein in the neighborhood of at least one labeled cell was selected. Cells were imaged prior to bleaching using a Zeiss LSM 510 DUO inverted, high-speed confocal microscope equipped with a three-channel and Meta detector and an LCI-Plan Neofluor 63× lens. A single spot in the analyzed cell was repeatedly bleached with 20 iterations using a 488-nm laser line (75 to 100% output). After each bleaching cycle, two pictures were collected. One FLIP experiment was completed after 10 cycles of repeated bleaching and image acquisition. The Zeiss ZEN 2010 software was used to analyze the fluorescence loss on the mitochondria of the selected cell. Additionally, an unbleached control cell was monitored during the measurement and used to exclude any photobleaching events that may occur during image acquisition.

Confocal Microscopy. HCT116 wild-type cells were seeded on coverslips coated with Poly-L-lysine (Sigma-Aldrich) in McCoy's 5A medium. After 48 h incubation, cells were transfected using Turbofect (Thermo Fisher Scientific) according to manufacturer's instructions. Then, cells were incubated with MitoTracker Deep Red FM (Thermo Fisher Scientific) for 10 min at 37 °C and fixed with 4% paraformaldehyde (PFA) for 10 min at room temperature. Finally, samples were mounted in Vectashield mounting medium (Linaris) and imaged using a ZEISS LSM 510 DUO with inverted microscope Axiovert 200 equipped with 488 and 633 nm lasers lines and a 63× PlanFluor lens.

Whole-Cell Lysis, Subcellular Fractionation, and In-Organelle Retrotranslocation Assay. Cells without ectopic protein expression were harvested, washed with phosphate-buffered saline (PBS), and incubated in cell lysis buffer (20 mM Tris pH7.4, 100 mM NaCl, 1 mM EDTA, 0.5% Triton X-100, and protease inhibitor mix) for 15 min on ice. After clearing the whole-cell extracts by centrifugation at 15,000 × *g* for 10 min at 4 °C, the resulting supernatants were either used in caspase 3/7 activity assays or subjected to acetone precipitation. Dried precipitation pellets were boiled in sodium dodecyl sulfate (SDS) sample buffer for 5 min at 95 °C and subsequently analyzed via SDS-PAGE and Western blot.

For subcellular fractionation into cytosolic and heavy membrane fractions cells were harvested, washed with PBS, and cell pellets resuspended in SEM buffer (10 mM Hepes pH 7.2, 250 mM sucrose) supplemented with protease inhibitors. After 10 min incubation on ice, cells were broken by two rounds of 10 passages through a 25G needle (Braun) fitted on a 1-mL syringe (Braun). After each round, the lysate was cleared from debris and unbroken cells by centrifugation for 5 min at 1,000 × *g*, and the supernatant of both steps was collected and pooled. The suspension was centrifuged at 10,000 × *g* at 4 °C for 10 min. The resulting pellet, representing the heavy membrane fraction, was washed two times in SEM buffer and one time in KCl buffer (125 mM KCl, 4 mM MgCl2, 5 mM Na_2HPO_4, 5 mM succinate, 0.5 mM EGTA, 15 mM Hepes–KOH, and pH 7.4), supplemented with protease inhibitors. The supernatant, representing the cytosolic fraction, was cleared at 150,000 × *g* at 4 °C for 30 min. The cytosolic fraction was acetone-precipitated, the pellets of both fractions boiled for 5 min at 95 °C in SDS sample buffer, and applied to SDS-PAGE and Western blot analysis. The in-organelle retrotranslocation assays were performed as previously described (28).

Mitochondrial Outer Membrane Permeabilization (MOMP) Assay. Isolated mitochondria of HCT116 wild-type cells without ectopic protein expression were preincubated with either 10 μM Cyclosporin A or 50 μM DIDS (Sigma) for 30 min at 4 °C, followed by a 10 min incubation at 37 °C with or without 1 nM tBID (R&D Systems). Controls containing the same amount of solvent were incubated at 37 °C in parallel.

Isolated mitochondria of MEF wild-type and MEF Bax/Bak DKO were incubated with 25, 100, or 250 μM of selected peptides for 1 h at 37 °C. As control, mitochondria were incubated with the solvent either on ice or at 37 °C. Subsequently, mitochondria and supernatant were separated at 13,000 × *g* at 4 °C for 5 min, and both fractions were subjected to Western blot analysis.

Clonogenic Survival Assay. HCT116 cells were seeded in 6-well plates. Cells were treated with either TRAIL (0.01 ng/μl to 1 ng/μl), Actinomycin D (0.01 μM to 1 μM), or Doxorubicin (0.01 μM to 1 μM) in the presence or the absence of 12 μM CLZ, 10 μM Cyclosporin A, or 50 μM DIDS for 24 h. Cells incubated with inhibitor solvent served as control. After an additional 24 h, recovery cells were replated in a 1:800 dilution. After 7 d incubation, surviving colonies were fixed with 4% PFA in PBS and stained with 1% methylene blue in 50% methanol. Colony numbers were determined via particle count using ImageJ software (NIH) and normalized to solvent controls.

Caspase 3/7 Activity Assay. HCT116 cells were treated with either TRAIL (0.03 ng/μl, 0.1 ng/μl, and 0.3 ng/μl), hexameric FasL (1 ng/mL, 3 ng/mL, and 10 ng/mL), Actinomycin D (0.1 μM, 0.3 μM, and 1 μM), or Doxorubicin (0.1 μM, 0.3 μM, and 1 μM) in the presence or the absence of 12 μM CLZ, 10 μM cyclosporin A, or 50 μM DIDS for 24 h. U2OS wild-type cells were treated with 0.3 ng/μL TRAIL (Sigma-Aldrich) for 4 h or with 1 μM Actinomycin D or 5 μM Doxorubicin for 16 h.

HCT116 BCL-2allKO cells were transfected with 250 ng pcDNA3.1-BAX, 2 μg pcDNA3.1-BCL-xL, and 1 μg pcDNA3.1-tBid or Bim plasmid for 16 h. Cells were treated in parallel with either 12 μM CLZ or solvent (dimethylsulfoxide [DMSO]). To test the inhibitory effect of hexokinase overexpression, HCT116 BCL-2allKO cells were transfected with 250 ng pcDNA3.1-BAX plasmid alone or cotransfected with either 250 ng pcDNA3.1 BCL-x_L or 4.5 μg pcDNA3.1-HK1 or -HK2 plasmid for 6 h.

At indicated time points, caspase-3/7 measurements were performed as described before (13). Whole-cell lysate was incubated with caspase 3/7 substrate (BD Pharmingen) in 100 mM Hepes, pH 7.4 and 2 mM dithiothreitole (DTT) for 60 min at 37 °C. Generation of the fluorescent caspase 3/7 substrate cleavage product was measured for 40 times at 2-min intervals with an excitation wavelength of 380 nm and an emission wavelength of 460 nm at 30 °C. The slope of the linear substrate cleavage reaction kinetic was determined and normalized to the protein concentration, as measured by Bradford assay (Roth).

HCT116 BCL-2allKO cells were seeded 1 d prior to transfection. HCT116 BCL-2allKO cells were transfected with 250 ng pcDNA3.1-BAX, 500 ng YFP-tBID, and 250 ng pcDNA3.1 BCL-xL plasmid or cotransfected with either 4.5 μg pcDNA3.1-HK1 or -HK2 or 4.5 μg pcDNA3.1-HK1 or -HK2 tail (aa 1 to 12) plasmid for 6 h.

Analysis of Native Protein Complexes. Isolated mitochondria were solubilized in 2% digitonin buffer (20 mM Tris·HCl, pH 7.4, 50 mM NaCl, 0.1 mM EDTA, 10% [vol/vol] glycerol, 2% [wt/vol] digitonin, and 1 mM phenylmethylsulfonylfluoride [PMSF]) at 4 °C for 30 min. Insoluble material was removed by centrifugation (13,000 × *g*, 5 min, 4 °C), and the mitochondrial extracts were applied to blue native PAGE (46). Mitochondrial protein complexes were separated using 4 to 13% continuous polyacrylamide gradient gels and were subsequently blotted onto a polyvinylidendifluoride (PVDF) membrane for Western blot analysis.

BioID Assay. HCT116 cells were transfected with pcDNA3-mycBioID-BAX plasmid for 24 h in the presence of 50 μM biotin and 10 μM QVD, resulting in myc-tagged BirA-BAX fusion expression. Cells were harvested, washed with PBS, and the cell pellet was lysed in SEM buffer (10 mM Hepes, pH7.2 and 250 mM sucrose) containing 0.2% Triton X-100 and complete proteinase inhibitor mix (Roche). Cell lysate was cleared via centrifugation at 120,000 × *g* at 4 °C for 30 min, applied to a concentrator column (Vivaspin 3000 molecular weight cut-off (MWCO), GE Healthcare) and washed by passing 14 volumes of washing buffer (100 mM Tris HCl, pH 8.0, 150 mM NaCl, 5 mM EDTA, 0.1% Triton X-100, and complete proteinase inhibitor mix, Roche) through the concentrator column. After separating an input sample, (2.5%) the remaining lysate was incubated with streptavidin agarose beads (Thermo Fisher) at 4 °C overnight. Then beads were washed four times with washing buffer and boiled in SDS sample buffer. Input and bead samples were resolved on a 10% SDS-PAGE and analyzed via Western blot for the indicated proteins.

Hexokinase Knockdown. HCT116 wild-type cells were seeded one day prior to transfection. Cells were transfected using Lipofectamine 2000 reagent (Life Technologies) according to manufacturer's instructions. Cotransfection with 200 nM HK1 siRNA (Thermo Fisher Scientific) and 100 nM HK2 siRNA or with the corresponding control siRNA (Cell Signaling Technology; Thermo Fisher Scientific) were performed. Cells were cultivated for two days before the cells were treated with 0,03 ng/μl TRAIL for 1h.

Immunoprecipitation. HCT116 BAX/BAK DKO cells were transfected with an empty cDNA3-mycBioID plasmid or cDNA3-mycBioID-BAX plasmids (wild-type, dC, 63–65A, dBH3) or YFP-tBid, YFP-Bim with and without BCL-x_L plasmid as indicated. When stated, cells were treated with 25 μM CLZ (Sigma-Aldrich) or solvent control (DMSO) for 4 h. Cells were harvested and washed with PBS prior to lysis in immunoprecipitation (IP)–solubilization buffer (20 mM Tris, pH

7.4, 50 mM NaCl, 10% glycerol, and 0.1 mM EDTA) supplemented with 2% digitonin (MATRIX BioScience GmbH) and proteinase inhibitors. After 20 min incubation on ice, cells were passaged though a 1-mL syringe (Braun) with a 25G needle (Braun). The cell debris was cleared (15,000 × *g*, 10 min, 4 °C) and 2.5% of the supernatant were used as input. The lysis was incubated with washed protein A Sepharose cl-4B beads (GE Healthcare) and GFP antibody (Novus) or Myc beads (C-myc [9E10] Santa Cruz), at 4 °C overnight. The following day, the beads were washed five times with IP-solubilization buffer (20 mM Tris, pH 7.4, 50 mM NaCl, 10% glycerol, and 0.1 mM EDTA), supplemented with 0,02% digitonin and proteinase inhibitors after centrifugation at 350 × *g*, 3 min, and 4 °C. Beads were boiled in SDS sample buffer, and input and IP samples were analyzed by Western blot.

Tetramethylrhodamine, Ethyl Ester (TMRE) Staining. HCT BCL2nullKO cells were transfected with 250 ng of pEGFP-BAX and 1.5 μg of pYFP and 250 ng pcDNA3.1 BCL-xL plasmid or cotransfected with either 4.5 μg pcDNA3.1-HK1 or -HK1dTMD plasmid. Cells were incubated in 100 nM TMRE for 30 min prior to haverst by trypsination after 6 h. Flow cytometry was performed with a BD LSRFortessa using the FACSDiva software (BD Biosciences) measuring the GFP-signal (laser 488 nm, channel 510/20 nm) and the TMRE (PE) signal (laser 561 nm, channel 586/15 nm) collecting 1×10^4 events per sample. Data analysis was performed using FlowJo version 10.2 (BD Biosciences).

Data Availability. All study data are included in the article and/or *SI Appendix*.

ACKNOWLEDGMENTS. We thank R. Youle (NIH, Bethesda) for HCT116 BAX/BAK DKO, S. Jakobs (TMPI, Göttingen) for U2OS cells, W. Craigen (Baylor College of Medicine, Houston) for VDAC2 KO MEFs, H. Ardehali (Northwestern University, Chicago) for pEGFP-HK1, P. Schneider (University of Lausanne) and A. Rensing-Ehl (University of Freiburg) for Fc-FasL, and S. Tait (Beatson Institute, Glasgow) for pEGFP-PUMA. This work is supported by the Emmy Noether program and the Sonderforschungsbereich 746 of the German Research Council (Deutsche Forschungsgemeinschaft), the Else Kröner Fresenius Foundation, the Wilhelm Sander Foundation, the Spemann Graduate School of Biology and Medicine (GSC-4), the Ministry for Science, Research and Arts of the State of Baden-Wuerttemberg, the Centre for Biological Signalling Studies (EXC-294) funded by the Excellence Initiative of the German Federal and State Governments, and the Max Planck Society. X.L. has been supported by the NIH (Grant R01GM118437).

1. J. E. Sulston, H. R. Horvitz, Post-embryonic cell lineages of the nematode, Caenorhabditis elegans. *Dev. Biol.* **56**, 110–156 (1977).
2. A. Zychlinsky, M. C. Prevost, P. J. Sansonetti, Shigella flexneri induces apoptosis in infected macrophages. *Nature* **358**, 167–169 (1992).
3. C. Clavería, G. Giovinazzo, R. Sierra, M. Torres, Myc-driven endogenous cell competition in the early mammalian embryo. *Nature* **500**, 39–44 (2013).
4. R. J. Youle, A. Strasser, The BCL-2 protein family: Opposing activities that mediate cell death. *Nat. Rev. Mol. Cell Biol.* **9**, 47–59 (2008).
5. C. Pop, G. S. Salvesen, Human caspases: Activation, specificity, and regulation. *J. Biol. Chem.* **284**, 21777–21781 (2009).
6. R. S. Hotchkiss, A. Strasser, J. E. McDunn, P. E. Swanson, Cell death. *N. Engl. J. Med.* **361**, 1570–1583 (2009).
7. S. J. Korsmeyer *et al*., Pro-apoptotic cascade activates BID, which oligomerizes BAK or BAX into pores that result in the release of cytochrome c. *Cell Death Differ.* **7**, 1166–1173 (2000).
8. K. Huang *et al*., BH3-only proteins target BCL-xL/MCL-1, not BAX/BAK, to initiate apoptosis. *Cell Res.* **29**, 942–952 (2019).
9. F. Llambi *et al*., A unified model of mammalian BCL-2 protein family interactions at the mitochondria. *Mol. Cell* **44**, 517–531 (2011).
10. X. Roucou, S. Montessuit, B. Antonsson, J.-C. Martinou, Bax oligomerization in mitochondrial membranes requires tBid (caspase-8-cleaved Bid) and a mitochondrial protein. *Biochem. J.* **368**, 915–921 (2002).
11. F. Edlich, The great migration of Bax and Bak. *Mol. Cell. Oncol.* **2**, e995029 (2015).
12. F. Edlich *et al*., Bcl-x(L) retrotranslocates Bax from the mitochondria into the cytosol. *Cell* **145**, 104–116 (2011).
13. F. Todt *et al*., Differential retrotranslocation of mitochondrial Bax and Bak. *EMBO J.* **34**, 67–80 (2015).
14. F. Reichenbach *et al*., Mitochondrial BAX determines the predisposition to apoptosis in human AML. *Clin. Cancer Res.* **23**, 4805–4816 (2017).
15. K. Funk *et al*., BAX redistribution induces apoptosis resistance and selective stress sensitivity in human HCC. *Cancers (Basel)* **12**, 1437 (2020).
16. E. C. Cheung, R. L. Ludwig, K. H. Vousden, Mitochondrial localization of TIGAR under hypoxia stimulates HK2 and lowers ROS and cell death. *Proc. Natl. Acad. Sci. U.S.A.* **109**, 20491–20496 (2012).
17. H.-J. Lee *et al*., Non-proteolytic ubiquitination of Hexokinase 2 by HectH9 controls tumor metabolism and cancer stem cell expansion. *Nat. Commun.* **10**, 2625 (2019).
18. P. Mergenthaler *et al*., Mitochondrial hexokinase II (HKII) and phosphoprotein enriched in astrocytes (PEA15) form a molecular switch governing cellular fate depending on the metabolic state. *Proc. Natl. Acad. Sci. U.S.A.* **109**, 1518–1523 (2012).
19. A. Ahmad *et al*., Elevated expression of hexokinase II protects human lung epithelial-like A549 cells against oxidative injury. *Am. J. Physiol. Lung Cell. Mol. Physiol.* **283**, L573–L584 (2002).
20. J. M. Bryson, P. E. Coy, K. Gottlob, N. Hay, R. B. Robey, Increased hexokinase activity, of either ectopic or endogenous origin, protects renal epithelial cells against acute oxidant-induced cell death. *J. Biol. Chem.* **277**, 11392–11400 (2002).
21. D. J. Roberts, V. P. Tan-Sah, J. M. Smith, S. Miyamoto, Akt phosphorylates HK-II at Thr-473 and increases mitochondrial HK-II association to protect cardiomyocytes. *J. Biol. Chem.* **288**, 23798–23806 (2013).
22. D. Palmieri *et al*., Analyses of resected human brain metastases of breast cancer reveal the association between up-regulation of hexokinase 2 and poor prognosis. *Mol. Cancer Res.* **7**, 1438–1445 (2009).
23. A. Wolf *et al*., Hexokinase 2 is a key mediator of aerobic glycolysis and promotes tumor growth in human glioblastoma multiforme. *J. Exp. Med.* **208**, 313–326 (2011).
24. S. A. Kwee, B. Hernandez, O. Chan, L. Wong, Choline kinase alpha and hexokinase-2 protein expression in hepatocellular carcinoma: Association with survival. *PLoS One* **7**, e46591 (2012).
25. S. Abu-Hamad, H. Zaid, A. Israelson, E. Nahon, V. Shoshan-Barmatz, Hexokinase-I protection against apoptotic cell death is mediated via interaction with the voltage-dependent anion channel-1: Mapping the site of binding. *J. Biol. Chem.* **283**, 13482–13490 (2008).
26. N. Majewski *et al*., Hexokinase-mitochondria interaction mediated by Akt is required to inhibit apoptosis in the presence or absence of Bax and Bak. *Mol. Cell* **16**, 819–830 (2004).
27. K. J. Roux, D. I. Kim, M. Raida, B. Burke, A promiscuous biotin ligase fusion protein identifies proximal and interacting proteins in mammalian cells. *J. Cell Biol.* **196**, 801–810 (2012).
28. J. Lauterwasser, F. Fimm-Todt, F. Edlich, Assessment of dynamic BCL-2 protein shuttling between outer mitochondrial membrane and cytosol. *Methods Mol. Biol.* **1877**, 151–161 (2019).
29. J. Lauterwasser *et al*., The porin VDAC2 is the mitochondrial platform for Bax retrotranslocation. *Sci. Rep.* **6**, 32994 (2016).
30. J. G. Pastorino, N. Shulga, J. B. Hoek, Mitochondrial binding of hexokinase II inhibits Bax-induced cytochrome c release and apoptosis. *J. Biol. Chem.* **277**, 7610–7618 (2002).
31. V. Andreu-Fernández *et al*., Bax transmembrane domain interacts with prosurvival Bcl-2 proteins in biological membranes. *Proc. Natl. Acad. Sci. U.S.A.* **114**, 310–315 (2017).
32. V. Andreu-Fernández *et al*., The C-terminal domains of apoptotic BH3-only proteins mediate their insertion into distinct biological membranes. *J. Biol. Chem.* **291**, 25207–25216 (2016).
33. K. L. O'Neill, K. Huang, J. Zhang, Y. Chen, X. Luo, Inactivation of prosurvival Bcl-2 proteins activates Bax/Bak through the outer mitochondrial membrane. *Genes Dev.* **30**, 973–988 (2016).
34. F. Chiara *et al*., Hexokinase II detachment from mitochondria triggers apoptosis through the permeability transition pore independent of voltage-dependent anion channels. *PLoS One* **3**, e1852 (2008).
35. F. Wilfling *et al*., BH3-only proteins are tail-anchored in the outer mitochondrial membrane and can initiate the activation of Bax. *Cell Death Differ.* **19**, 1328–1336 (2012).
36. J. Lopez *et al*., Mito-priming as a method to engineer Bcl-2 addiction. *Nat. Commun.* **7**, 10538 (2016).
37. K. A. Sarosiek *et al*., BID preferentially activates BAK while BIM preferentially activates BAX, affecting chemotherapy response. *Mol. Cell* **51**, 751–765 (2013).
38. F. Masson, F. Kupresanin, A. Mount, A. Strasser, G. T. Belz, Bid and Bim collaborate during induction of T cell death in persistent infection. *J. Immunol.* **186**, 4059–4066 (2011).
39. M. Certo *et al*., Mitochondria primed by death signals determine cellular addiction to antiapoptotic BCL-2 family members. *Cancer Cell* **9**, 351–365 (2006).
40. T. Ni Chonghaile *et al*., Pretreatment mitochondrial priming correlates with clinical response to cytotoxic chemotherapy. *Science* **334**, 1129–1133 (2011).
41. Y. Guo, S. M. Srinivasula, A. Druilhe, T. Fernandes-Alnemri, E. S. Alnemri, Caspase-2 induces apoptosis by releasing proapoptotic proteins from mitochondria. *J. Biol. Chem.* **277**, 13430–13437 (2002).
42. J.-P. Upton *et al*., Caspase-2 cleavage of BID is a critical apoptotic signal downstream of endoplasmic reticulum stress. *Mol. Cell. Biol.* **28**, 3943–3951 (2008).
43. C. Bogner, B. Leber, D. W. Andrews, Apoptosis: Embedded in membranes. *Curr. Opin. Cell Biol.* **22**, 845–851 (2010).
44. J. F. Lovell *et al*., Membrane binding by tBid initiates an ordered series of events culminating in membrane permeabilization by Bax. *Cell* **135**, 1074–1084 (2008).
45. F. Todt, Z. Cakir, F. Reichenbach, R. J. Youle, F. Edlich, The C-terminal helix of Bcl-x(L) mediates Bax retrotranslocation from the mitochondria. *Cell Death Differ.* **20**, 333–342 (2013).
46. H. Schägger, G. von Jagow, Blue native electrophoresis for isolation of membrane protein complexes in enzymatically active form. *Anal. Biochem.* **199**, 223–231 (1991).